A Random Field Approach to Reliability Analysis With Random and Interval Variables

Zhen Hu
Department of Mechanical and Aerospace Engineering,
Missouri University of Science and Technology,
272 Toomey Hall,
400 West 13th Street,
Rolla, MO 65409-0500
e-mail: zh4hd@mst.edu

Xiaoping Du
Professor
Department of Mechanical and Aerospace Engineering,
Missouri University of Science and Technology,
272 Toomey Hall,
400 West 13th Street,
Rolla, MO 65409-0500
e-mail: dux@mst.edu

Interval variables are commonly encountered in design, especially in the early design stages when data are limited. Thus, reliability analysis (RA) should deal with both interval and random variables and then predict the lower and upper bounds of reliability. The analysis is computationally intensive, because the global extreme values of a limit-state function with respect to interval variables must be obtained during the RA. In this work, a random field approach is proposed to reduce the computational cost with two major developments. The first development is the treatment of a response variable as a random field, which is spatially correlated at different locations of the interval variables. Equivalent reliability bounds are defined from a random field perspective. The definitions can avoid the direct use of the extreme values of the response. The second development is the employment of the first-order reliability method (FORM) to verify the feasibility of the random field modeling. This development results in a new random field method based on FORM. The new method converts a general response variable into a Gaussian field at its limit state and then builds surrogate models for the autocorrelation function and reliability index function with respect to interval variables. Then, Monte Carlo simulation is employed to estimate the reliability bounds without calling the original limit-state function. Good efficiency and accuracy are demonstrated through three examples. [DOI: 10.1115/1.4030437]

Keywords: random field, interval variable, epistemic uncertainty, reliability analysis

1 Introduction

The major task of RA is to predict reliability in the design stage. Because of this advantage, RA has been used in many applications, such as those of automobile vehicles [1], wind/hydrokinetic turbines [2], and airplanes [3]. The RA requires a known limit-state function, which specifies the functional relationship between input variables and output variables (responses), and the joint probability distribution of the input variables.

In many applications, especially in the early design stages, the data of some input variables are too limited to fit probability distributions. For this situation, the fuzzy set [4], evidence theory [5], random matrix theory [6–8], and intervals [9,10] are employed to model the uncertainty of the input variables. Interval variables are used for the highest degree of uncertainty—only the lower and upper bonds of an input variable are available. For instance, the contact resistance in the vehicle crash [11] and the tolerances of the dimension of a new product [12] are examples of interval variables. As a result, the input variables of a limit-state function may contain both random and interval variables, and the reliability is therefore also bounded within its minimum and maximum values.

Many methods are available for RA with the mixture of random and interval variables. For example, Jiang et al. [13] developed a RA method based on a hybrid uncertain model. In their model, parameters such as means and standard deviations of some random variables are described as interval variables. Adduri and Penmetsa [14] investigated the method of approximating the bounds of structural system reliability in the presence of interval variables. Luo et al. [15,16] developed an iterative procedure to obtain the worst-case points of interval variables and the most probable point (MPP) using a probability and convex set model. Penmetsa and Grandhi [17] used function approximation methods to improve the efficiency of RA with random and interval variables. By combining simulation process with interval analysis (IA), Zhang et al. [18] proposed an interval Monte Carlo method to estimate the interval probability of failure. In order to perform reliability-based design optimization for problems with interval variables, Du et al. developed a sequential single-loop (SSL) procedure [19,20]. To improve the stability of SSL, Jiang et al. designed a new algorithm [12].

Although many reliability methods can accommodate interval variables as reviewed earlier, there are still some challenges that need to be resolved. First, the RA requires global extreme values of a response with respect to interval variables. As a result, the RA usually involves two loops. In the inner loop, global optimization is used to find the extreme values of the response with respect to interval variables, whereas the outer loop is responsible for RA with respect to random variables. Even though single-loop procedures have been proposed [12,19,20], efficient global optimization is still indispensable. Second, the extreme values of the response may be highly nonlinear with respect to interval variables and may have multiple MPPs, which may lead to large errors if the first-order and second-order reliability methods (FORM and SORM) are used based on the extreme values of the response. Third, most of the current methods only focus on the worst-case reliability, or the lower bound of the reliability. To understand the uncertainty in the reliability, one may also want to know the upper bound of the reliability.

The objective of this work is to deal with the aforementioned challenges by developing a new random field approach for RA with both random and interval variables. The contributions and significance of the new method are as follows: (1) This work develops a new way to model the reliability with random and interval variables. A response variable is viewed as a random field that is spatially correlated at different locations of interval variables. This allows for using random field methodologies to calculate the lower and upper bounds of reliability. (2) A new FORM-based random field approach is developed for the RA with random and interval variables. The method transforms the general random field of the response into a Gaussian field, which is then expanded as a function of a number of Gaussian variables. The use of global optimization is

Manuscript received May 26, 2014; final manuscript received October 10, 2014; published online September 30, 2015. Assoc. Editor: Alba Sofi.

thus avoided, and the use of Monte Carlo simulation (MCS) then becomes possible to obtain both the maximum and minimum values of the reliability simultaneously. (3) An efficient algorithm of the Kriging model method is developed to build the mean and autocorrelation functions of the transformed Gaussian field. The transformed Gaussian field is therefore fully defined with good accuracy and efficiency.

The reminder of this paper is organized as follows: Section 2 reviews the methods of RA with both random and interval variables. Section 3 discusses the idea of RA with a random field approach, followed by the numerical implementation in Sec. 4. Three examples are presented in Sec. 5. Conclusions and future work are given in Sec. 6.

2 Review of RA With Random and Interval Variables

A response variable G may be a function of random variables $\mathbf{X} = [X_i]_{i=1,\ldots,n}$ and interval variables $\mathbf{Y} = [Y_j]_{j=1,\ldots,m}$. If only $\mathbf{Y}$ exists, the response is given by

$$G = g(\mathbf{Y}) \tag{1}$$

where $\mathbf{Y} \in [\underline{\mathbf{Y}}, \bar{\mathbf{Y}}]$; $\underline{\mathbf{Y}} = [\underline{Y}_j]_{j=1,m}$ and $\bar{\mathbf{Y}} = [\bar{Y}_j]_{j=1,m}$ are the lower and upper bounds, respectively.

G is also an interval, whose lower and upper bounds are defined by

$$\underline{G} = \min_{\mathbf{Y}\in[\underline{\mathbf{Y}},\bar{\mathbf{Y}}]} \{g(\mathbf{Y})\} \tag{2}$$

and

$$\bar{G} = \min_{\mathbf{Y}\in[\underline{\mathbf{Y}},\bar{\mathbf{Y}}]} \{g(\mathbf{Y})\} \tag{3}$$

respectively. Figure 1 shows an interval response for a two-dimensional case.

If both $\mathbf{X}$ and $\mathbf{Y}$ exist, the response is given by

$$G = g(\mathbf{X}, \mathbf{Y}) \tag{4}$$

The extreme responses $\bar{G}$ and $\underline{G}$ are now random variables. If a failure occurs when $G < e$, where e is a limit state, the probability of failure is defined by

$$p_f = \Pr\{g(\mathbf{X}, \mathbf{Y}) < e\} \tag{5}$$

Eq. (5) indicates that $\bar{G}(\mathbf{X})$ and $\underline{G}(\mathbf{X})$ are the best-case response and worst-case response, respectively.

The corresponding best-case and worst-case probabilities are then given by

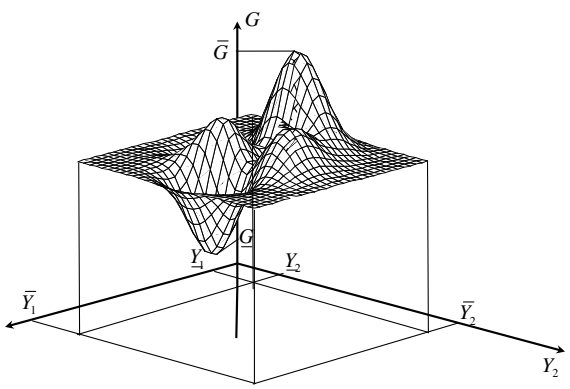

Fig. 1 Limit-state function with interval variables

$$\underline{p}_f = \Pr\{\bar{G}(\mathbf{X}) < e\} = \Pr\Big\{\max_{\mathbf{Y}\in[\underline{\mathbf{Y}},\bar{\mathbf{Y}}]} \{g(\mathbf{X}, \mathbf{Y})\} < e\Big\} \tag{6}$$

and

$$\bar{p}_f = \Pr\{\underline{G}(\mathbf{X}) < e\} = \Pr\Big\{\min_{\mathbf{Y}\in[\underline{\mathbf{Y}},\bar{\mathbf{Y}}]} \{g(\mathbf{X}, \mathbf{Y})\} < e\Big\} \tag{7}$$

As obtaining the extreme responses $\bar{G}$ and $\underline{G}$ requires the global optimization on $[\underline{\mathbf{Y}}, \bar{\mathbf{Y}}]$, calculating $\underline{p}_f$ and $\bar{p}_f$ is extremely costly in computation. Next, we briefly review two common types of RA methods for problems with both random and interval variables.

The first type includes methodologies that combine RA, such as FORM, and IA. If FORM is used for RA, $\mathbf{X}$ is transformed into standard normal variables $\mathbf{U}$ [21], and the transformation is denoted by $\mathbf{X} = T[\mathbf{U}]$. Then the reliability indices ($\bar{\beta}$ and $\underline{\beta}$) are obtained by

$$\begin{cases} \bar{\beta} = \min\limits_{\mathbf{U}} \sqrt{\mathbf{U}\mathbf{U}^T} \\ \text{s.t.} \max\limits_{\mathbf{Y}} \{g(T[\mathbf{U}], \mathbf{Y})\} = e \end{cases} \tag{8}$$

and

$$\begin{cases} \underline{\beta} = \min\limits_{\mathbf{U}} \sqrt{\mathbf{U}\mathbf{U}^T} \\ \text{s.t.} \min\limits_{\mathbf{Y}} \{g(T[\mathbf{U}], \mathbf{Y})\} = e \end{cases} \tag{9}$$

Then, the probabilities of failure are given by

$$\underline{p}_f = \Phi(-\bar{\beta}) \tag{10}$$

and

$$\bar{p}_f = \Phi(-\underline{\beta}) \tag{11}$$

The optimal point from Eqs. (8) or (9) is called a MPP, denoted by $\bar{\mathbf{u}}^*$ for Eq. (8) and $\underline{\mathbf{u}}^*$ for Eq. (9).

Evaluating the equality constraint functions in Eqs. (8) and (9) requires global optimization on $\mathbf{Y} \in [\underline{\mathbf{Y}}, \bar{\mathbf{Y}}]$, and the entire analysis needs a double-loop optimization process, thereby being computationally expensive. The following are some examples of the first-type methodologies. An iterative procedure [15] using a probability and convex mixed model was reported in [16]. By applying the performance measure approach, the method transforms the nested double-loop optimization problem into an approximate single-loop minimization problem. With a similar principle, an SSL method, as mentioned in Sec. 1, decouples the double-loop procedure into an SSL [19,20].

After the SSL method, Jiang et al. [12] proposed an equivalent model method to improve the robustness of the single-loop algorithm. The method demonstrates that solving Eq. (9) is equivalent to solving a general MPP problem after treating the interval variables as uniformly distributed random variables [12]. The method is efficient compared with other single-loop methods, but similar to other methods that use FORM; its accuracy may not be good. When G is highly nonlinear with respect to $\mathbf{Y}$, the linearization of the limit-state function at the MPP with respect to $\mathbf{Y}$ will result in large errors. The aforementioned methods also need to be performed twice to obtain the lower and upper bounds of p_f, thereby increasing the computational cost.

The second type of methodologies uses design of experiments. A surrogate model of $G = g(\mathbf{X}, \mathbf{Y})$ is built first, and then the extreme probabilities of failure are estimated by MCS. In this group of methods, interval variables are usually treated as variables following uniform distributions. For instance, Zhuang and Pan approximated limit-state functions with interval variables using the Kriging method [22]. Li et al. [23] also used the Kriging method to build a surrogate model for a bilevel limit-state function with only random variables. The model is constructed by applying the probability theory for random variables and a nonprobabilistic reliability method for interval variables. Yoo and Lee [24] performed

the sensitivity analysis with respect to interval variables, and surrogate models are employed to approximate the reliability. Zhang and Hosder [25] expanded the random and interval variables using the stochastic expansion methods.

Although all the aforementioned methods can deal with both random and interval variables, their accuracy and efficiency may still need to be improved. From a different perspective, this work views limit-state functions with interval variables as general random fields, and this leads to a new modeling and analysis method that can potentially improve the efficiency and accuracy of the RA.

3 Reliability Modeling From a Random Field Perspective

We now show that the RA problem can be approached from a random field perspective, and we also discuss the advantages of doing so. A random field is essentially a spatial-variant random variable [26]. In other words, its distribution changes at different locations, and the random variable at one location is usually dependent on that at another location. Random fields have been used to describe spatially varying and dependent quantities, such as mechanical properties of materials, including Young's modulus, Poisson's ratio, and yield stress [27], as well as temperature, deformation, and surface forces.

For example, the thickness, D, of a metal sheet shown in Fig. 2 is a random field. At a specific location (y_1, y_2), D is a random variable with a specific distribution. The distribution of D is different at another location (y_1', y_2'), and $D(y_1, y_2)$ is dependent on $D(y_1', y_2')$. In this case, the spatial variables are the Y_1- and Y_2-coordinates.

We can consider the response $G = g(\mathbf{X}, \mathbf{Y})$ as a random field. The reasons are as follows:

- G is a random variable. If $\mathbf{Y}$ is fixed at $\mathbf{y}$, $G = g(\mathbf{X}, \mathbf{y})$ is random, and its distribution is determined by $g(\cdot)$ and the joint probability density function (PDF) of $\mathbf{X}$.
- The distribution of G changes with respect to $\mathbf{Y}$. The distribution at $\mathbf{y}$ may be different from that at $\mathbf{y}'$ because $G = g(\mathbf{X}, \mathbf{y})$ may be different from $G' = g(\mathbf{X}, \mathbf{y}')$ as shown in the metal sheet example in Fig. 2 and another two-dimensional example in Fig. 3.
- $G = g(\mathbf{X}, \mathbf{y})$ and $G' = g(\mathbf{X}, \mathbf{y}')$ may be dependent because they share common random variables $\mathbf{X}$.
- For any given $\mathbf{X} = \mathbf{x}$, $G = g(\mathbf{x}, \mathbf{Y})$ is a realization of the field.

For the aforementioned reasons, G is indeed a random field whose spatial variables are intervals $\mathbf{Y}$. G is a general nonstationary random field, as its distributions are not constant (varying with respect to $\mathbf{Y}$) and the dimensions of the spatial variable $\mathbf{Y}$ are m, maybe greater than two or three.

The random field perspective allows us to use random field methodologies to calculate the probability of failure. To do so, we redefine the bounds of the probability of failure as follows:

$$\underline{p}_f = \Pr\{G = g(\mathbf{X}, \mathbf{y}) < e, \quad \forall\ \mathbf{y} \in [\underline{\mathbf{Y}}, \bar{\mathbf{Y}}]\} \tag{12}$$

where $\forall$ stands for "for all." The minimum probability of failure is the probability that all the interval bounds are completely in the failure region

$$\bar{p}_f = \Pr\{G = g(\mathbf{X}, \mathbf{y}) < e, \quad \exists\ \mathbf{y} \in [\underline{\mathbf{Y}}, \bar{\mathbf{Y}}]\} \tag{13}$$

where $\exists$ stands for "there exists at least one." The maximum probability is the probability that the interval bounds intersect the failure region.

Let us examine why the new definitions are equivalent to the original definitions given in Eqs. (6) and (7). Recall that the original maximum probability of failure $\bar{p}_f$ is defined as $\bar{p}_f = \Pr\{\underline{G} = \min_{\mathbf{Y} \in [\underline{\mathbf{Y}}, \bar{\mathbf{Y}}]} \{g(\mathbf{X}, \mathbf{Y})\} < e\}$ in Eq. (7). The definition is equivalent to the definition given in Eq. (13). The reason is that the two events $A = \{\underline{G}(\mathbf{X}) < e\}$ in Eq. (7) and $B = \{G = g(\mathbf{X}, \mathbf{y}) < e, \exists \mathbf{y} \in [\underline{\mathbf{Y}}, \bar{\mathbf{Y}}]\}$ in Eq. (13) are equivalent. For event B, at least at one point of $\mathbf{Y}$, $G < e$. There are two cases:

- *Case 1*: There is only one point $\mathbf{y}'$ where $G < e$, and event B becomes $B = \{g(\mathbf{X}, \mathbf{y}') < e\}$. This mean that at other points on $[\underline{\mathbf{Y}}, \bar{\mathbf{Y}}]$, except at $\mathbf{y}'$, $G \geq e$. Then $\mathbf{y}'$ is the point where G is minimum, or $\underline{G}(\mathbf{X}) = g(\mathbf{X}, \mathbf{y}')$. Thus, event A becomes $A = \{\underline{G} = g(\mathbf{X}, \mathbf{y}') < e\}$. Event A is therefore equivalent to event B.
- *Case 2*: There are multiple points $[\mathbf{y}_i']_{i=1,h}$ where $G < e$. Event B is then an intersection expressed by $B = \cap_{i=1}^{h} \{g(\mathbf{X}, \mathbf{y}_i') < e\}$. At all the other points on $[\underline{\mathbf{Y}}, \bar{\mathbf{Y}}]$, $G \geq e$. Let $\mathbf{y}'' \in [\mathbf{y}_i']_{i=1,h}$ be the point where G is minimum, or $\underline{G} = g(\mathbf{X}, \mathbf{y}'')$. Event B can be rewritten as $B = \{\min_{\mathbf{y}_i'} g(\mathbf{X}, \mathbf{y}_i') < e\} = \{\underline{G} = g(\mathbf{X}, \mathbf{y}'') < e\}$, which is equivalent to event A.

Similarly, the original minimum probability of failure $\underline{p}_f$, defined as $\underline{p}_f = \Pr\{\bar{G} = \max_{\mathbf{Y} \in [\underline{\mathbf{Y}}, \bar{\mathbf{Y}}]} \{g(\mathbf{X}, \mathbf{Y})\} < e\}$ in Eq. (6), is equivalent to the definition given in Eq. (12) because event $C = \{\bar{G} < e\}$ in Eq. (8) is equivalent to event $D = \{g(\mathbf{X}, \mathbf{y}) < e, \forall \mathbf{y} \in [\underline{\mathbf{Y}}, \bar{\mathbf{Y}}]\}$ in Eq. (12). The equivalence holds because $g(\mathbf{X}, \mathbf{y}) \leq \bar{G}$ for all $\mathbf{y} \in [\underline{\mathbf{Y}}, \bar{\mathbf{Y}}]$, and thus $C = \{\bar{G} < e\} = \{g(\mathbf{X}, \mathbf{y}) \leq \bar{G} < e, \forall \mathbf{y} \in [\underline{\mathbf{Y}}, \bar{\mathbf{Y}}]\} = D$.

The advantages of the new definitions are multifold. First, it avoids the direct use of the global responses with respect to interval variables. The elimination of global optimization can improve the computational efficiency significantly for responses that are highly nonlinear with respect to interval variables. Second, defining the probability of failure with a random field approach enables us to use existing random field methodologies to estimate the bounds of the probability of failure differently, and the methodologies are potentially more accurate and efficient than the traditional methods. Third, as discussed in Sec. 4, the definitions also make it easy to integrate the traditional reliability methods and a random field approach to solve the problems with both random and interval variables.

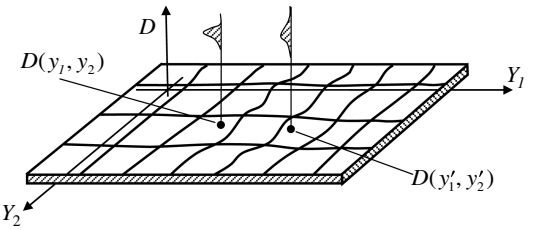

Fig. 2 Random field thickness of a metal sheet

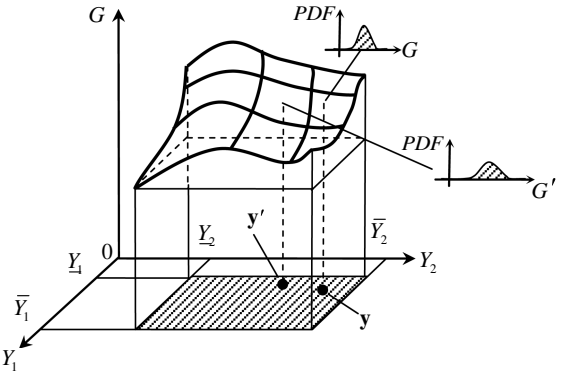

Fig. 3 Responses with both random and interval variables

As the second task of this work, we demonstrate the feasibility of the proposed random approach by developing a new numerical procedure that employs FORM and a random field expansion method. The details are given in Sec. 4.

4 FORM Using Random Field Approach

As indicated in Eqs. (12) and (13), the lower and upper bounds of p_f can be calculated by considering G as a random field. Directly using the random field G, however, is difficult because it is in general a non-Gaussian and nonstationary random field, and no analytical solutions exist.

In this work, we use FORM to transform G into a Gaussian random field $\tilde{G}$. A similar strategy has been applied to the time-dependent RA involving stochastic processes [28], which can be considered as one interval variable. Herein, we extend the strategy to the problem with more interval variables. Although $\tilde{G}$ is a Gaussian field, its extreme value is not analytically available, as it is in general a nonstationary random field. For this reason, we use a simulation method, which is feasible because the original limit-state function is no longer needed once $\tilde{G}$ is available.

The simulation of $\tilde{G}$ usually involves discretizing the random field with respect to the spatial variables, or interval variables, particularly in this study. In the following sections, we first introduce the discretization methods of a Gaussian field and then discuss the details of the implementation procedure.

4.1 Discretization Methods of a Gaussian Random Field.

The discretization of a Gaussian field has been extensively studied. There are three groups of discretization methods, including the point discretization method, the average discretization method, and the series expansion method [27]. A review of the discretization methods is available in [29]. A simulation method only uses a finite set of random variables with a sufficiently large size of the set. In this work, we use the expansion optimal linear estimation method (EOLE), because it is more efficient than the other approximation methods for general problems when exact solutions of the eigenvalue problem are not available [29]. Note that the simulation methods are not limited to EOLE; other methods can also be used.

Theoretically, a Gaussian field consists of an infinite set of correlated Gaussian random variables, and a simulation method only uses a finite set of random variables. For this reason, EOLE expands a Gaussian field $\tilde{G}$ into a series of finite random variables. Let $\tilde{G}$ have its mean function $\mu(\mathbf{y})$, standard deviation function $\sigma(\mathbf{y})$, and autocorrelation function $\rho(\mathbf{y},\mathbf{y}')$. After discretizing $[\underline{\mathbf{Y}},\bar{\mathbf{Y}}]$ into p points $[\mathbf{y}_i]_{i=1,p}$, $\tilde{G}$ is expanded as

$$\tilde{G} \approx \mu(\mathbf{y}) + \sigma(\mathbf{y}) \sum_{i=1}^{r} \frac{\xi_i}{\sqrt{\eta_i}} \boldsymbol{\varphi}_i^T \boldsymbol{\rho}_G(\mathbf{y}), \quad \forall\ \mathbf{y} \in [\underline{\mathbf{Y}},\bar{\mathbf{Y}}] \tag{14}$$

where η_i and $\boldsymbol{\varphi}_i^T$ are the eigenvalues and eigenvectors of the correlation matrix $\boldsymbol{\rho}$ with element $\rho_{ij} = \rho(\mathbf{y}_i,\mathbf{y}_j)$, $i,j = 1,2,\ldots,p$, $\boldsymbol{\rho}_G(\mathbf{y}) = [\rho(\mathbf{y},\mathbf{y}_1), \rho(\mathbf{y},\mathbf{y}_2), \ldots, \rho(\mathbf{y},\mathbf{y}_p)]^T$, and $r \le p$ is the number of terms of expansion. Note that the eigenvalues η_i are sorted in decreasing order.

As discussed earlier, a Gaussian field can be completely characterized and discretized once we know its mean value function $\mu(\mathbf{y})$, standard deviation function $\sigma(\mathbf{y})$, and autocorrelation function $\rho(\mathbf{y},\mathbf{y}')$. Next, we discuss how to obtain $\tilde{G}$ and its associated functions.

4.2 Construction of an Equivalent Gaussian Field $\tilde{G}$.

To use EOLE in Eq. (14), we need to transform the general random field G into an equivalent Gaussian field $\tilde{G}$. We do so by using FORM.

4.2.1 Transformation by FORM. FORM has been widely used in RA with only random variables [30–32]. It can also be used for problems with both random and interval variables. It requires searching for the MPP. For a given $\mathbf{y} \in [\underline{\mathbf{Y}},\bar{\mathbf{Y}}]$, the MPP of $g(\mathbf{X},\mathbf{y})$ is obtained by

$$\begin{cases} \min\limits_{\mathbf{u}} \sqrt{\mathbf{U}\mathbf{U}^T} \\ \text{s.t. } G = g(T(\mathbf{U}),\mathbf{y}) \le e \end{cases} \tag{15}$$

where $T(\mathbf{U})$ is an operator that transforms standard normal variables $\mathbf{U}$ to $\mathbf{X}$ [21].

After the MPP search, $g(T(\mathbf{U}),\mathbf{y})$ is linearized at the MPP point $\mathbf{u}^*(\mathbf{y})$ using Taylor's series expansion as follows:

$$g(T(\mathbf{U}),\mathbf{y}) \approx \hat{g}(\mathbf{U},\mathbf{y}) = g(\mathbf{u}^*(\mathbf{y}),\mathbf{y}) + \nabla g(\mathbf{u}^*(\mathbf{y}),\mathbf{y})(\mathbf{U}-\mathbf{u}^*(\mathbf{y}))^T \tag{16}$$

where

$$\nabla g(\mathbf{u}^*(\mathbf{y}),\mathbf{y}) = \left(\left.\frac{\partial g(\mathbf{U},\mathbf{y})}{\partial U_1}\right|_{\mathbf{u}^*(\mathbf{y})}, \left.\frac{\partial g(\mathbf{U},\mathbf{y})}{\partial U_2}\right|_{\mathbf{u}^*(\mathbf{y})}, \ldots, \left.\frac{\partial g(\mathbf{U},\mathbf{y})}{\partial U_n}\right|_{\mathbf{u}^*(\mathbf{y})} \right) \tag{17}$$

The accuracy loss of the Taylor expansion is minimal at the MPP, where $g(\mathbf{u}^*(\mathbf{y}),\mathbf{y}) = e$, for $\mathbf{y} \in [\underline{\mathbf{Y}},\bar{\mathbf{Y}}]$. We then have

$$\Pr\{G = g(\mathbf{X},\mathbf{y}) < e\} \approx \Pr\{\nabla g(\mathbf{u}^*(\mathbf{y}),\mathbf{y})(\mathbf{U}-\mathbf{u}^*(\mathbf{y}))^T < 0\} \tag{18}$$

Eq. (18) is rewritten as

$$\Pr\{G = g(\mathbf{X},\mathbf{y}) < e\} \approx \Pr\left\{ \frac{\nabla g(\mathbf{u}^*(\mathbf{y}),\mathbf{y})}{\|\nabla g(\mathbf{u}^*(\mathbf{y}),\mathbf{y})\|} \mathbf{U}^T < \frac{\nabla g(\mathbf{u}^*(\mathbf{y}),\mathbf{y})}{\|\nabla g(\mathbf{u}^*(\mathbf{y}),\mathbf{y})\|} \mathbf{u}^*(\mathbf{y})^T \right\} \tag{19}$$

At the MPP point, we also have $\frac{\nabla g(\mathbf{u}^*(\mathbf{y}),\mathbf{y})}{\|\nabla g(\mathbf{u}^*(\mathbf{y}),\mathbf{y})\|} = -\frac{\mathbf{u}^*(\mathbf{y})}{\|\mathbf{u}^*(\mathbf{y})\|}$; Eq. (19) then becomes

$$\Pr\{G = g(\mathbf{X},\mathbf{y}) < e\} \approx \Pr\left\{ -\frac{\mathbf{u}^*(\mathbf{y})}{\|\mathbf{u}^*(\mathbf{y})\|} \mathbf{U}^T < -\frac{\mathbf{u}^*(\mathbf{y})}{\|\mathbf{u}^*(\mathbf{y})\|} \mathbf{u}^*(\mathbf{y})^T \right\} \tag{20}$$

By defining $\boldsymbol{\alpha}(\mathbf{y}) = -\frac{\mathbf{u}^*(\mathbf{y})}{\|\mathbf{u}^*(\mathbf{y})\|}$ and $\beta(\mathbf{y}) = \|\mathbf{u}^*(\mathbf{y})\|$, we have

$$\Pr\{G = g(\mathbf{X},\mathbf{y}) < e\} \approx \Pr\{\boldsymbol{\alpha}(\mathbf{y})\mathbf{U}^T < -\beta(\mathbf{y})\} \tag{21}$$

Thus, the probability if failure is

$$\Pr\{G = g(T(\mathbf{U}),\mathbf{y}) \le e\} \approx \Pr\{\tilde{G} = \tilde{g}(\mathbf{U},\mathbf{y}) = \boldsymbol{\alpha}(\mathbf{y})\mathbf{U}^T + \beta(\mathbf{y}) < 0\} \tag{22}$$

The mean and standard deviation functions of $\tilde{G}$ are then given by

$$\mu_{\tilde{G}}(\mathbf{y}) = E\{\boldsymbol{\alpha}(\mathbf{y})\mathbf{U}^T\} + \beta(\mathbf{y}) = \beta(\mathbf{y}) \tag{23}$$

$$\sigma_{\tilde{G}}(\mathbf{y}) = \|\boldsymbol{\alpha}(\mathbf{y})\| = 1 \tag{24}$$

where $E\{\cdot\}$ stands for expectation.

Eqs. (23) and (24) indicate that for any $\mathbf{y} \in [\underline{\mathbf{Y}},\bar{\mathbf{Y}}]$, the equivalent response $\tilde{G}$ is a Gaussian random variable with mean $\mu_{\tilde{G}}(\mathbf{y}) = \beta(\mathbf{y})$ and standard deviation $\sigma_{\tilde{G}}(\mathbf{y}) = 1$.

4.2.2 Properties of $\tilde{G}$. If the MPP search is performed at two points, $\mathbf{y},\mathbf{y}' \in [\underline{\mathbf{Y}},\bar{\mathbf{Y}}]$, we have

$$\Pr\{G = g(T(\mathbf{U}),\mathbf{y}) \le e\} \approx \Pr\{\tilde{G}(\mathbf{y}) = \boldsymbol{\alpha}(\mathbf{y})\mathbf{U}^T + \beta(\mathbf{y}) < 0\} \tag{25}$$

$$\Pr\{G = g(T(\mathbf{U}), \mathbf{y}) \le e\} \approx \Pr\{\tilde{G}(\mathbf{y}') = \boldsymbol{\alpha}(\mathbf{y}')\mathbf{U}^T + \beta(\mathbf{y}') < 0\} \tag{26}$$

Since $\tilde{G}(\mathbf{y})$ and $\tilde{G}(\mathbf{y}')$ share common random variables $\mathbf{U}$, they are generally correlated. The correlation coefficient between $\tilde{G}(\mathbf{y})$ and $\tilde{G}(\mathbf{y}')$ is given by

$$\rho(\mathbf{y}, \mathbf{y}') = \frac{E\{\tilde{G}(\mathbf{y})\tilde{G}(\mathbf{y}')\} - E\{\tilde{G}(\mathbf{y})\}E\{\tilde{G}(\mathbf{y}')\}}{\sigma_{\tilde{G}(\mathbf{y})}\sigma_{\tilde{G}(\mathbf{y}')}} \tag{27}$$

The aforementioned expression can be simplified as

$$\rho(\mathbf{y}, \mathbf{y}') = \boldsymbol{\alpha}(\mathbf{y})\boldsymbol{\alpha}(\mathbf{y}')^T, \mathbf{y}, \mathbf{y}' \in [\underline{\mathbf{Y}}, \bar{\mathbf{Y}}] \tag{28}$$

From the previous discussions, we know that $\tilde{G}$ has he following properties:

- $\tilde{G}$ is a Gaussian random variable for any given $\mathbf{y} \in [\underline{\mathbf{Y}}, \bar{\mathbf{Y}}]$.
- The distribution of $\tilde{G}$ changes with respect to $\mathbf{y}$ as its mean $\mu_{\tilde{G}}(\mathbf{y}) = \beta(\mathbf{y})$ is a function of $\mathbf{y}$.
- For any two points $\mathbf{y}, \mathbf{y}' \in [\underline{\mathbf{Y}}, \bar{\mathbf{Y}}]$, $\tilde{G}(\mathbf{y})$, and $\tilde{G}(\mathbf{y}')$ are in general correlated with the correlation coefficient given in Eq. (28).

The properties of $\tilde{G}$ show that $\tilde{G}$ is indeed a Gaussian field with mean $\mu_{\tilde{G}}(\mathbf{y}) = \beta(\mathbf{y})$, standard deviation $\sigma_{\tilde{G}}(\mathbf{y}) = 1$, and autocorrelation function $\rho(\mathbf{y}, \mathbf{y}')$. By performing FORM at every point $\mathbf{y} \in [\underline{\mathbf{Y}}, \bar{\mathbf{Y}}]$, we can map the random field G into an equivalent Gaussian field $\tilde{G}$.

Based on the equivalence given in Eq. (22), the minimum and maximum probabilities of failure are then computed with $\tilde{G}$ as follows:

$$\begin{aligned} \underline{p}_f &= \Pr\{G = g(\mathbf{X}, \mathbf{y}) < e, \quad \forall\ \mathbf{y} \in [\underline{\mathbf{Y}}, \bar{\mathbf{Y}}]\} \\ &\approx \Pr\{\tilde{G} = \tilde{g}(\mathbf{U}, \mathbf{y}) < 0, \quad \forall\ \mathbf{y} \in [\underline{\mathbf{Y}}, \bar{\mathbf{Y}}]\} \end{aligned} \tag{29}$$

$$\begin{aligned} \bar{p}_f &= \Pr\{G = g(\mathbf{X}, \mathbf{y}) < e, \quad \exists\ \mathbf{y} \in [\underline{\mathbf{Y}}, \bar{\mathbf{Y}}]\} \\ &\approx \Pr\{\tilde{G} = \tilde{g}(\mathbf{U}, \mathbf{y}) < 0, \quad \exists\ \mathbf{y} \in [\underline{\mathbf{Y}}, \bar{\mathbf{Y}}]\} \end{aligned} \tag{30}$$

There are no close forms available for the probabilities given in Eqs. (29) and (30). To estimate these probabilities, a sampling-based method is presented based on the discretization of the equivalent Gaussian field.

4.3 Discretization of the Equivalent Random Field

4.3.1 Discretization of $\tilde{G}$. Assume that the functions of $\beta(\mathbf{y})$ and $\rho(\mathbf{y}, \mathbf{y}')$ are exactly known, the equivalent Gaussian field $\tilde{G}$ is then fully defined. The original limit-state function is no longer needed for the RA. $\tilde{G}$ is usually a nonstationary Gaussian field, and there is no analytical solution available to find whether there exists a particular point of $\mathbf{y}$ on $[\underline{\mathbf{Y}}, \bar{\mathbf{Y}}]$ when a failure occurs. For this reason, we need to approximate or discretize $\tilde{G}$ with respect to $\mathbf{Y}$ so that the sample points of $\mathbf{Y}$, where failure occurs, can be captured. As discussed in Sec. 4.1, there are many discretization methods available. Here, we use the EOLE [33] method.

We first generate s points for the interval variables on $[\underline{\mathbf{Y}}, \bar{\mathbf{Y}}]$ using the Hammersley sampling (HS) sampling method. Let the s points be $[\mathbf{y}_i]_{i=1,s}$; using the Kriging model of $\rho(\mathbf{y}, \mathbf{y}')$, we have the correlation matrix of these points as follows:

$$\boldsymbol{\Sigma} = \begin{pmatrix} \rho(\mathbf{y}_1, \mathbf{y}_1) & \rho(\mathbf{y}_1, \mathbf{y}_2) & \cdots & \rho(\mathbf{y}_1, \mathbf{y}_s) \\ \rho(\mathbf{y}_2, \mathbf{y}_1) & \rho(\mathbf{y}_2, \mathbf{y}_2) & \cdots & \rho(\mathbf{y}_2, \mathbf{y}_s) \\ \vdots & \vdots & \ddots & \vdots \\ \rho(\mathbf{y}_s, \mathbf{y}_1) & \rho(\mathbf{y}_s, \mathbf{y}_2) & \cdots & \rho(\mathbf{y}_s, \mathbf{y}_s) \end{pmatrix}_{s \times s} \tag{31}$$

where $\rho(\mathbf{y}_i, \mathbf{y}_j)$, $i, j = 1, s$, are correlation coefficients of $\tilde{G}(\mathbf{y}_i)$ and $\tilde{G}(\mathbf{y}_j)$, which are obtained by plugging $\mathbf{y}_i$ and $\mathbf{y}_j$ into the surrogate model $\rho(\mathbf{y}, \mathbf{y}')$.

Based on the correlation matrix and Eq. (14), $\tilde{G}$ is then discretized as

$$\tilde{G} \approx \beta(\mathbf{y}) + \sum_{i=1}^{s} \frac{Z_i}{\sqrt{\eta_i}} \varphi \boldsymbol{\varphi}_i^T \boldsymbol{\rho}_{\tilde{G}}(\mathbf{y}), \quad \forall\ \mathbf{y} \in [\underline{\mathbf{Y}}, \bar{\mathbf{Y}}] \tag{32}$$

where Z_i, $i = 1, s$, are independent standard normal variables, η_i and $\boldsymbol{\varphi}_i$ are eigenvalues and eigenvectors of the correlation matrix $\boldsymbol{\Sigma}$, and $\boldsymbol{\rho}_{\tilde{G}}(\mathbf{y}) = [\rho(\mathbf{y}, \mathbf{y}_1), \rho(\mathbf{y}, \mathbf{y}_2), \ldots, \rho(\mathbf{y}, \mathbf{y}_s)]^T$.

Upon the discretization of G, MCS can be performed by plugging random samples of Z_i, $i = 1, s$, and samples of $\mathbf{Y}$ into Eq. (32). Suppose n_{MCS} samples are generated for each random variable Z_i and n_y samples are generated for $\mathbf{Y}$ on $[\underline{\mathbf{Y}}, \bar{\mathbf{Y}}]$ using the HS method; we then have the following sampling matrix of G

$$\tilde{\mathbf{G}} = \begin{pmatrix} \tilde{G}(\mathbf{y}_1, 1) & \tilde{G}(\mathbf{y}_2, 1) & \cdots & \tilde{G}(\mathbf{y}_{n_y}, 1) \\ \tilde{G}(\mathbf{y}_1, 2) & \tilde{G}(\mathbf{y}_2, 2) & \cdots & \tilde{G}(\mathbf{y}_{n_y}, 2) \\ \vdots & \vdots & \ddots & \vdots \\ \tilde{G}(\mathbf{y}_1, n_{\text{MCS}}) & \tilde{G}(\mathbf{y}_2, n_{\text{MCS}}) & \cdots & \tilde{G}(\mathbf{y}_{n_y}, n_{\text{MCS}}) \end{pmatrix}_{n_{\text{MCS}} \times n_y} \tag{33}$$

Based on the sampling matrix, the bounds of probability of failure are estimated, which will be discussed in Sec. 4.4. From the discretization mentioned previously of the equivalent Gaussian random field, it can be found that $\beta(\mathbf{y})$ and $\rho(\mathbf{y}, \mathbf{y}')$ are required at each of the discretization point. If MPP searches are performed at each of the discretization point to obtain $\beta(\mathbf{y})$ and $\rho(\mathbf{y}, \mathbf{y}')$, it will be computationally expensive. To further improve the efficiency, we use surrogate models to reduce the number of MPP searches.

4.3.2 Surrogate Models of $\beta(\mathbf{y})$ and $\rho(\mathbf{y}, \mathbf{y}')$. As discussed in Sec. 4.2.2, if we perform the MPP search at $\mathbf{y}$, we obtain $\beta(\mathbf{y})$. If we also perform the MPP search at $\mathbf{y}'$, we obtain $\beta(\mathbf{y}')$ and $\rho(\mathbf{y}, \mathbf{y}')$. After the two MPP searches at $\mathbf{y}$ and $\mathbf{y}'$, we obtain $\beta(\mathbf{y})$, $\beta(\mathbf{y}')$, and $\rho(\mathbf{y}, \mathbf{y}')$. In this work, we use the Kriging model method [34], which determines the locations of $\mathbf{y}$ and $\mathbf{y}'$ iteratively without using uniformly distributed points of $\mathbf{y}$ and $\mathbf{y}'$. In this way, the number of MPP searches can be reduced.

The output of a Kriging model is assumed to be a stochastic process [34–36]. The Kriging model of a function $f(\mathbf{y})$ is given by [37–39]

$$\hat{f}(\mathbf{y}) = \mathbf{h}(\mathbf{y})^T \boldsymbol{\upsilon} + \varepsilon(\mathbf{y}) \tag{34}$$

where $\boldsymbol{\upsilon} = [\upsilon_1, \upsilon_2, \ldots, \upsilon_p]^T$ is a vector of unknown coefficients, $\mathbf{h}(\mathbf{y}) = [h_1(\mathbf{y}), h_2(\mathbf{y}), \ldots, h_p(\mathbf{y})]^T$ is a vector of regression functions, $\mathbf{h}(\mathbf{y})^T\boldsymbol{\upsilon}$ is the polynomial parts and the trend of prediction, and $\varepsilon(\mathbf{y})$ is usually assumed to be a Gaussian process with zero mean and covariance $\text{Cov}[\varepsilon(\mathbf{y}_i), \varepsilon(\mathbf{y}_j)]$.

The covariance between two points $\mathbf{y}_i$ and $\mathbf{y}_j$ is given by

$$\text{Cov}[\varepsilon(\mathbf{y}_i), \varepsilon(\mathbf{y}_j)] = \sigma_\varepsilon^2 R(\mathbf{y}_i, \mathbf{y}_j) \tag{35}$$

in which σ_ε^2 is the process variance and $R(\cdot, \cdot)$ is the correlation function. There exists a variety of correlation functions, such as the exponential function, Gaussian function, cubic function, and spline function. The most commonly used correlation function is the Gaussian correlation function, which is given by [34–39]

$$R(\mathbf{y}_i, \mathbf{y}_j) = \exp\left[-\sum_{k=1}^{n_d} a_k |\mathbf{y}_i^k - \mathbf{y}_j^k|^2\right] \tag{36}$$

where n_d is the number of design variables, a_k are the unknown correlation parameters, and $\mathbf{y}_i^k$ is the kth component of the sample $\mathbf{y}_i$.

With n_s training points, $[\mathbf{y}_i, f(\mathbf{y}_i)]_{i=1,2,\ldots,n_s}$, a correlation matrix $\mathbf{R}$ with element, $R(\mathbf{y}_i, \mathbf{y}_j)$, $i, j = 1, 2, \ldots, n_s$, will be obtained. Let $\mathbf{H} = [\mathbf{h}(\mathbf{y}_1)^T, \mathbf{h}(\mathbf{y}_2)^T, \ldots, \mathbf{h}(\mathbf{y}_{n_s})^T]^T$ and $\mathbf{F} = [f(\mathbf{y}_1), f(\mathbf{y}_2), \ldots, f(\mathbf{y}_{n_s})]^T$, the coefficient $\boldsymbol{\upsilon}$ is solved by

$$\boldsymbol{\upsilon} = (\mathbf{H}^T\mathbf{R}^{-1}\mathbf{H})^{-1}\mathbf{H}^T\mathbf{R}^{-1}\mathbf{F} \tag{37}$$

For a new point $\mathbf{y}$, the expected value of the prediction is given by

$$\hat{f}(\mathbf{y}) = \mathbf{h}(\mathbf{y})^T\boldsymbol{\upsilon} + \mathbf{r}(\mathbf{y})^T\mathbf{R}^{-1}(\mathbf{F} - \mathbf{H}\boldsymbol{\upsilon}) \tag{38}$$

where

$$\mathbf{r}(\mathbf{y}) = [R(\mathbf{y}, \mathbf{y}_1), R(\mathbf{y}, \mathbf{y}_2), \ldots, R(\mathbf{y}, \mathbf{y}_{n_s})] \tag{39}$$

The mean square error (MSE) of the prediction is given by [40]

$$\begin{aligned}\mathrm{MSE}(\mathbf{y}) = E\{[\hat{f}(\mathbf{y}) - f(\mathbf{y})]^2\} = \sigma_z^2\{1 - \mathbf{r}(\mathbf{y})^T\mathbf{R}^{-1}\mathbf{r}(\mathbf{y}) \\ + [\mathbf{H}^T\mathbf{R}^{-1}\mathbf{r}(\mathbf{y}) - \mathbf{h}(\mathbf{y})]^T(\mathbf{H}^T\mathbf{R}^{-1}\mathbf{H})^{-1} \\ \times [\mathbf{H}^T\mathbf{R}^{-1}\mathbf{r}(\mathbf{y}) - \mathbf{h}(\mathbf{y})]\end{aligned} \tag{40}$$

in which

$$\sigma_z^2 = \frac{(\mathbf{F} - \mathbf{H}\boldsymbol{\upsilon})^T\mathbf{R}^{-1}(\mathbf{F} - \mathbf{H}\boldsymbol{\upsilon})}{n_s} \tag{41}$$

The unknown parameters a_k, $k = 1, 2, \ldots, n$, are solved by maximizing the maximum likelihood estimator (MLE), which is given as follows:

$$\ln[(\mathbf{F}|\mathbf{R})] = -\frac{n_s \ln \sigma_z^2}{2} - \frac{\ln|\mathbf{R}|}{2} \tag{42}$$

where $|\mathbf{R}|$ is the determinant of $\mathbf{R}$.

Detailed derivations of aforementioned equations are available in [38,39,41,42], and a Kriging toolbox DACE is also available [40]. Herein, we focus on the application of the Kriging model for $\beta(\mathbf{y})$ and $\rho(\mathbf{y}, \mathbf{y}')$.

Even if $\beta(\mathbf{y})$ and $\rho(\mathbf{y}, \mathbf{y}')$ are two different functions, they share common input variables on $[\underline{\mathbf{Y}}, \bar{\mathbf{Y}}]$. The result of the MPP search for $\beta(\mathbf{y})$ can also be used for $\rho(\mathbf{y}, \mathbf{y}')$. We therefore construct surrogate models for $\beta(\mathbf{y})$ and $\rho(\mathbf{y}, \mathbf{y}')$ simultaneously. In addition, Eq. (28) gives $\rho(\mathbf{y}, \mathbf{y}') = 1$ for any $\mathbf{y} = \mathbf{y}'$. Taking advantage of these features of $\beta(\mathbf{y})$ and $\rho(\mathbf{y}, \mathbf{y}')$, we can design an efficient algorithm to create the surrogate models. Figure 4 shows such a procedure. The detailed steps are explained as follows:

Step 1 through Step 3: Create initial Kriging models

- *Step 1*: Generate evenly distributed initial samples $\mathbf{y}^s = [\mathbf{y}_i^s]_{i=1,\ldots,k}$ on $[\underline{\mathbf{Y}}, \bar{\mathbf{Y}}]$ using the HS sampling approach.
- *Step 2*: Obtain initial samples of $\boldsymbol{\beta}$ and $\boldsymbol{\rho}$ for surrogate models:
  1. Perform MPP searches at $\mathbf{y}_i^s$, $i = 1, k$, using the optimization model given in Eq. (15); obtain $\alpha(\mathbf{y}_i^s)$ and $\beta(\mathbf{y}_i^s)$.
  2. Obtain $\boldsymbol{\beta} = [\beta_i]_{i=1,\ldots,k}$, $\mathbf{yy}^s = [\mathbf{y}_i^s, \mathbf{y}_j^s]_{i,j=1,\ldots,k}$, and $\boldsymbol{\rho} = [\rho(\mathbf{y}_i^s, \mathbf{y}_j^s)]_{i,j=1,\ldots,k}$ using Eq. (30).
- *Step 3*: Construct the initial Kriging models of $\beta(\mathbf{y})$ and $\rho(\mathbf{y}, \mathbf{y}')$ using $\{\mathbf{y}^s, \boldsymbol{\beta}\}$ and $\{\mathbf{yy}^s, \boldsymbol{\rho}\}$, respectively.

Step 4 through Step 8: Update models and create final models

- *Step 4*: Identify the maximum MSE and the associated new sample point:
  1. Find the maximum MSEs of $\beta(\mathbf{y})$ and $\rho(\mathbf{y}, \mathbf{y}')$ using $[\mathbf{y}^\beta, \varepsilon_\beta^{\max}] = \arg\max_{\mathbf{y}\in[\mathbf{Y}^L, \mathbf{Y}^U]} \mathrm{MSE}_\beta(\mathbf{y})$ and $[(\mathbf{y}_1^\rho, \mathbf{y}_2^\rho), \varepsilon_\rho^{\max}] = \arg\max_{\mathbf{y}_1, \mathbf{y}_2\in[\mathbf{Y}^L, \mathbf{Y}^U]} \mathrm{MSE}_\rho(\mathbf{y}_1, \mathbf{y}_2)$, respectively.
  2. $\mathrm{MSE}_\beta(\mathbf{y})$ and $\mathrm{MSE}_\rho(\mathbf{y}_1, \mathbf{y}_2)$ are obtained from the outputs of the Kriging model based on Eq. (40) [40].
  3. If $\varepsilon_\rho^{\max} > \varepsilon_\beta^{\max}$, let $\varepsilon^{\max} = \varepsilon_\rho^{\max}$, $\mathbf{y}^{\text{new}} = [\mathbf{y}_1^\rho, \mathbf{y}_2^\rho]$; otherwise, let $\varepsilon^{\max} = \varepsilon_\beta^{\max}$, $\mathbf{y}^{\text{new}} = \mathbf{y}^\beta$.
- *Step 5*: Check convergence: If $\varepsilon^{\max} > \varepsilon_{\text{MSE}}$, go to next step; otherwise, obtain surrogate models of $\beta(\mathbf{y})$ and $\rho(\mathbf{y}, \mathbf{y}')$.
- *Step 6*: Perform MPP searches at $\mathbf{y}^{\text{new}}$ using the optimization model given in Eq. (15), and obtain $\boldsymbol{\alpha}(\mathbf{y}^{\text{new}})$ and $\beta(\mathbf{y}^{\text{new}})$.
- *Step 7*: Update $\mathbf{y}^s$, $\boldsymbol{\beta}$, $\mathbf{yy}^s$, and $\boldsymbol{\rho}$: $\mathbf{y}^s = [\mathbf{y}^s, \mathbf{y}^{\text{new}}]$, $\boldsymbol{\beta} = [\boldsymbol{\beta}, \beta(\mathbf{y}^{\text{new}})]$, $\mathbf{yy}^s = [\mathbf{y}_i^s, \mathbf{y}_j^s]_{i,j=1,\ldots,h}$, and $\boldsymbol{\rho} = [\rho(\mathbf{y}_i^s, \mathbf{y}_j^s)]_{i,j=1,\ldots,h}$, where h is the number of samples of $\mathbf{y}^s$.
- *Step 8*: Construct new Kriging models $\beta(\mathbf{y})$ and $\rho(\mathbf{y}, \mathbf{y}')$ using $\{\mathbf{y}^s, \boldsymbol{\beta}\}$ and $\{\mathbf{yy}^s, \boldsymbol{\rho}\}$, and then go to Step 4.

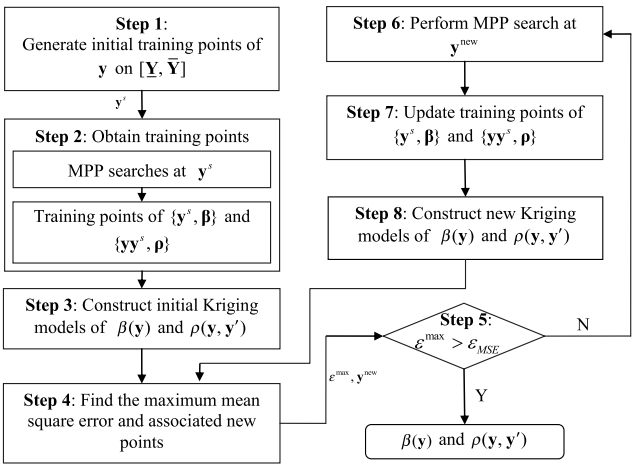

Fig. 4 Flowchart of constructing surrogate models of $\beta(\mathbf{y})$ and $\rho(\mathbf{y},\mathbf{y}')$

In Step 1, many sampling generation methods can be used, such as the random sampling method (RS) [43], the Latin hypercube sampling (LHS) method [44], and the HS method [45]. In this work, we use the HS method as it is capable of generating more evenly distributed samples than other methods. In Step 2, MPP searches are performed. To reduce the number of function calls, we should carefully select a good starting point for the MPP search. We pick the MPP that has been already obtained as the starting point. The MPP of the sample point, which is the closest to the current sample point $\mathbf{y}_i^s$, is selected as the starting point of $\mathbf{y}_i^s$. In Step 4, the maximum MSEs are used as the stopping criteria. As they are calculated by the Kriging models, there is no need to call the original limit-state function in this step. Any optimization methods can be used to determine the maximum MSEs, e.g., the DIRECT algorithm [46].

The numerical procedure shows that MPP searches are performed in Steps 2 and 6. At each training point of $\mathbf{y}$, the MPP search is performed. As a result, the total number of MPP searches is equal to the total number of training points of $\mathbf{y}$, including both the initial training points and the updated training points. If we consider creating the Kriging models as one loop and the MPP search as the other loop, the proposed method involves a double-loop procedure, but it is in general more efficient than the traditional double-loop method where the global optimization with respect to the interval variables is required. The new method eliminates the need of global optimization, thereby increasing computational efficiency. Note that we use the Kriging method to create the surrogate models of the mean and autocorrelation functions of the approximated Gaussian field, but other regression methods can also be used.

4.4 Reliability Analysis. To approximate the lower and upper bounds of the probability of failure, we first define the following indicator function:

$$F(i,j) = \begin{cases} 1, & \text{if } \tilde{G}(\mathbf{y}_j, i) < 0, i = 1, \ldots, n_{\text{MCS}}, j = 1, \ldots, n_Y \\ 0, & \text{otherwise} \end{cases} \tag{43}$$

According to Eqs. (29) and (30), $\underline{p}_f$ and $\bar{p}_f$ are then estimated by

$$\underline{p}_f \approx \frac{1}{n_{\text{MCS}}} \sum_{i=1}^{n_{\text{MCS}}} F^L(i) \tag{44}$$

$$\bar{p}_f \approx \frac{1}{n_{\text{MCS}}} \sum_{i=1}^{n_{\text{MCS}}} F^U(i) \tag{45}$$

where

$$F^L(i) = \begin{cases} 1, & \text{if } \sum_{j=1}^{n_Y} F(i,j) = n_Y \\ 0, & \text{otherwise} \end{cases} \tag{46}$$

$$F^U(i) = \begin{cases} 1, & \text{if } \sum_{j=1}^{n_Y} F(i,j) > 0 \\ 0, & \text{otherwise} \end{cases} \tag{47}$$

As indicated previously, with the new approach, $\underline{p}_f$ and $\bar{p}_f$ can be estimated simultaneously, and no global optimization with respect to the interval variables is required.

5 Examples

In this section, three examples are used to demonstrate the accuracy and efficiency of the proposed method. Each example is solved using the following four methods:

- The proposed random field approach, denoted by *Random Field*.
- The direct Kriging model method, denoted by *Direct Kriging*, which constructs a surrogate model of the response with respect to both random and interval variables and then uses MCS to calculate the extreme probabilities of failure.
- The equivalent model method proposed by Jiang et al. [12], denoted by *Equivalent MPP*.
- The direct MCS.

The solution from MCS with a sufficiently large sample size is used as a benchmark for the accuracy comparison, and the efficiency is measured by the number of the limit-state function calls for the response variable.

5.1 Mathematical Example. The model is given in Eq. (48) with four random variables and one interval variable defined in Table 1. The response function is nonlinear with respect to the interval variable.

$$g(\mathbf{X}, \mathbf{Y}) = -10.5 + 2.1X_1^2X_2\sin^2(Y_1 + 0.3) - 2X_3(Y_1 + 0.3) + (X_1 + X_4)(Y_1 - 0.7)^2 \tag{48}$$

The limit state is $e = -10$, and thus the probability of failure is given by

$$p_f = \Pr\{g(\mathbf{X}, \mathbf{Y}) < -10\} \tag{49}$$

where $\mathbf{X} = [X_i]_{i=1,4}$.

In Table 1, parameters 1 and 2 are the mean and standard deviation of a random variable, respectively. For an interval variable, the two parameters are the lower and upper bounds, respectively.

Building the surrogate models for $\beta(\mathbf{y})$ and $\rho(\mathbf{y}, \mathbf{y}')$ is critical for the proposed random field approach, and we now show the results of the two models in Figs. 5 and 6. The initial training points and added training points of $\mathbf{Y}$ are also plotted in the figures. For surrogate models of $\beta(\mathbf{y})$ and $\rho(\mathbf{y}, \mathbf{y}')$, the regression function is chosen to be constant ($\mathbf{h}(\mathbf{y}) = 1$) and the Gaussian correlation function is used as the correlation function. The initial point, lower bound, and upper bound for the optimization of unknown coefficients a_k are $a_k^0 = 10$, $a_k^l = 0.1$, and $a_k^u = 500$, respectively.

Table 1 Variables and parameters of Example 1

Variable	Parameter 1	Parameter 2	Distribution
X_1	2	0.2	Normal
X_2	3	0.3	Normal
X_3	3.5	0.35	Normal
X_4	2	0.4	Normal
Y_1	0	1.5	Interval

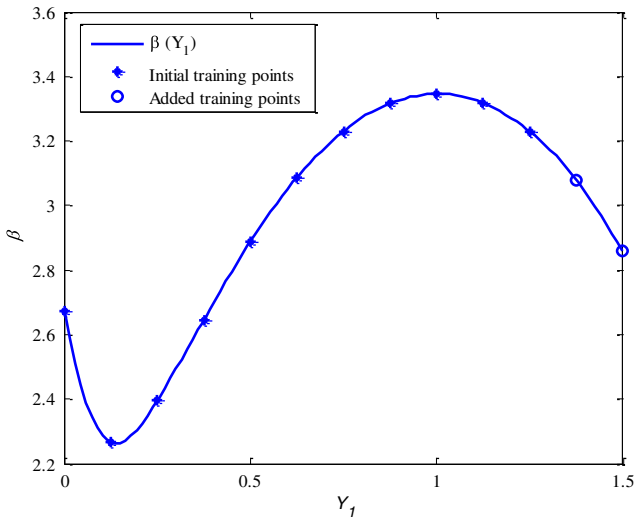

Fig. 5 Surrogate model of $\beta(\mathbf{y})$

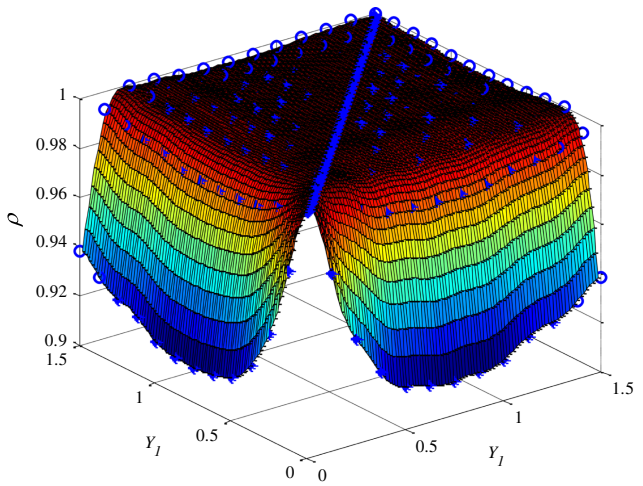

Fig. 6 Surrogate model of $\rho(\mathbf{y},\mathbf{y}')$

Table 2 Results of Example 1

Method	$[\underline{p}_f, \bar{p}_f]$	$[\underline{\varepsilon}, \bar{\varepsilon}]$ (%)	NOF
Random field	$[4.21 \times 10^{-4}, 1.25 \times 10^{-2}]$	[0.94, 2.8]	335
Direct Kriging	$[3.50 \times 10^{-4}, 1.08 \times 10^{-2}]$	[17.65, 16.18]	500
Equivalent MPP	$[\text{N/A}, 1.0 \times 10^{-2}]$	[N/A, 22.48]	242
MCS	$[4.25 \times 10^{-4}, 1.29 \times 10^{-2}]$	N/A	4×10^8

The convergence criterion of the two surrogate models is $\varepsilon_{\text{MSE}} = 1 \times 10^{-4}$. Thirteen training points in total were used, and thus, the MPP search was performed 13 times. The results show that both $\beta(\mathbf{y})$ and $\rho(\mathbf{y}, \mathbf{y}')$ are nonlinear with respect to the interval variable.

Recall that the probability of failure p_f can be evaluated with the equivalent Gaussian random field $\tilde{G}$ through Eqs. (29) and (30). With $\beta(\mathbf{y})$ and $\rho(\mathbf{y}, \mathbf{y}')$ available, $\tilde{G}$ is fully defined. Then $\tilde{G}$ could be expanded, followed by MCS. The final results are given in Table 2, where NOF is the number of function calls. The *Random field* approach evaluated the limit-state function 335 times.

For a fair comparison, we used 500 training points for the direct Kriging method to generate a direct Kriging model for the response with respect to $\mathbf{X}$ and Y. The number of the training points was much higher than that used by the random field approach. The range of a random variable X was set to $[\mu_{\mathbf{X}} - 5\sigma_{\mathbf{X}}, \mu_{\mathbf{X}} + 5\sigma_{\mathbf{X}}]$, and the training points were generated by the HS method. The equivalent MPP method and MCS were also executed.

All the results are given in Table 2. $\underline{\varepsilon}$ and $\bar{\varepsilon}$ are the percentage errors of the lower and upper probabilities of failure with respect to the MCS solutions, respectively. The results show that the proposed random field approach is more efficient and accurate than the direct Kriging method. Note that the equivalent MPP method used the fewest number of function calls, but this does not mean that it is more efficient than the random field approach because it calculated only the upper probability of failure, and its accuracy is much worse.

5.2 Cantilever Tube. The cantilever tube example shown in Fig. 7 is modified from Ref. [19]. The component is subjected to three forces F_1, F_2, and P, as well as a torque T. A failure occurs when the maximum von Mises stress $\sigma_{\max}$ is larger than the yield strength S_y. The limit-state function is given by

$$G = g(\mathbf{X}, \mathbf{Y}) = S_y - \sigma_{\max} \tag{50}$$

where $\mathbf{X} = [S_y, t, d, F_1, F_2, P, T]$, $\mathbf{Y} = [\theta_1, \theta_2]$, and $\sigma_{\max}$ is given by

$$\sigma_{\max} = \sqrt{\sigma_x^2 + 3\tau_{zx}^2} \tag{51}$$

Table 3 Variables of Example 2

Variable	Parameter 1	Parameter 2	Distribution
t (mm)	6	0.2	Normal
d (mm)	43	0.2	Normal
F_1 (N)	1000	50	Normal
F_2 (N)	1700	80	Normal
P (N)	1000	50	Normal
T (Nm)	350	20	Normal
S_y (MPa)	360	0	Normal
θ_1 (°)	−5	10	Interval
θ_2 (°)	−10	6	Interval

in which

$$\sigma_x = \frac{P}{A} + \frac{M}{I} \tag{52}$$

$$\tau_{xz} = \frac{[2T + F_1 d \sin(\theta_1) - F_2 d \sin(\theta_2)]d}{8I} \tag{53}$$

$$I = \frac{\pi}{64}[d^4 - (d - 2t)^4] \tag{54}$$

$$A = \frac{\pi}{4}[d^2 - (d - 2t)^2] \tag{55}$$

and

$$M = F_1 L_1 \cos(\theta_1) - F_2 L_2 \cos(\theta_2) \tag{56}$$

where $L_1 = 120$ mm and $L_2 = 60$ mm.

All the input variables are given in Table 3. Parameters 1 and 2 have the same meanings as those in Example 1. The probability of failure is defined by $p_f = \Pr\{G = g(\mathbf{X}, \mathbf{Y}) < 0\}$, and the limit state is $e = 0$. This problem involves seven independent random variables and two interval variables.

Figure 8 shows the maximum von Mises stress with respect to interval variables θ_1 and θ_2, where all the random variables are fixed at their mean values. The surface is quite nonlinear. Given that the maximum von Mises stress is part of the response, the response is therefore also highly nonlinear with respect to the interval variables.

The parameters of the Kriging model for constructing surrogate models of $\beta(\mathbf{y})$ and $\rho(\mathbf{y}, \mathbf{y}')$ are the same as those of Example 1. The RA results of all the methods are provided in Table 4. For the direct Kriging model method, we used 400 training points, which are more than the training points used by the random field approach.

The results also show the high accuracy and efficiency of the random field method.

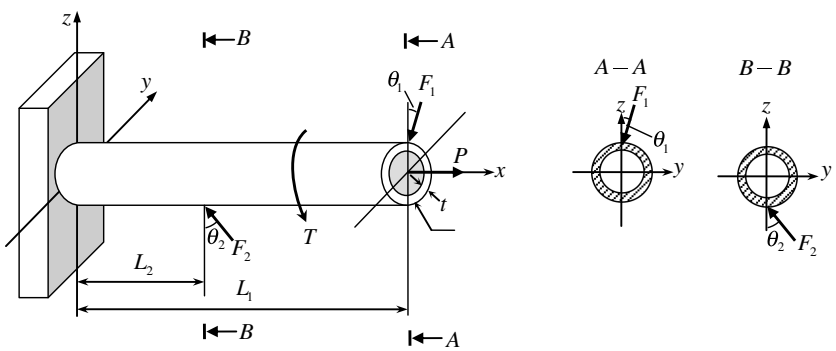

Fig. 7 Cantilever tube

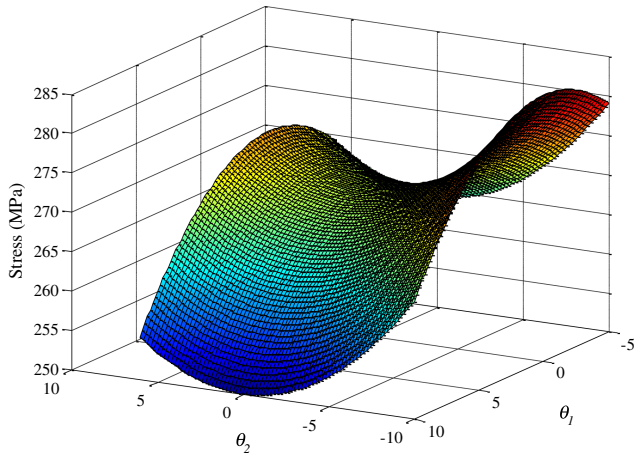

Fig. 8 Maximum von Mises stress of the tube for a given θ_1 and θ_2

Table 4 Results of Example 2

Method	$[\underline{p}_f, \bar{p}_f]$	$[\underline{\varepsilon}, \bar{\varepsilon}]$ (%)	NOF
Random field	$[2.07 \times 10^{-4}, 9.86 \times 10^{-4}]$	[1.90, 1.89]	371
Direct Kriging	$[1.2 \times 10^{-4}, 7.10 \times 10^{-3}]$	[43.13, 576.19]	400
Equivalent MPP	$[\text{N/A}, 5.64 \times 10^{-4}]$	[N/A, 43.62]	257
MCS	$[2.11 \times 10^{-4}, 1.0 \times 10^{-3}]$	N/A	3×10^9

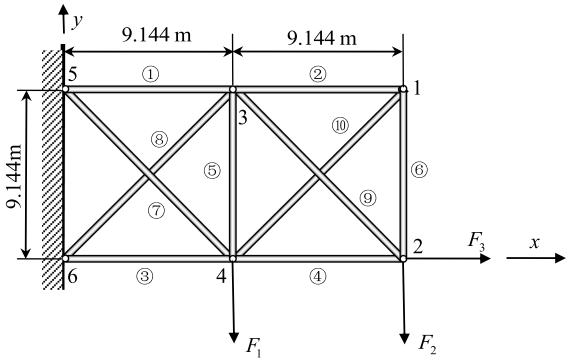

Fig. 9 Ten-bar aluminum truss

5.3 Ten-Bar Aluminum Truss. This example is modified from Refs. [12,16,47]. As shown in Fig. 9, a ten-bar aluminum truss is subjected to forces F_1, F_2, and F_3. The vertical displacement of joint 2 is of interest. Its allowable value is $d_{\max} = 0.046$ m. The Young's modulus of the material is $E = 68.948$ GPa. The lengths of the horizontal and vertical bars are all $L = 9.144$ m.

The probability of failure is given by

$$p_f = \Pr\{G = g(\mathbf{X}, \mathbf{Y}) = d_{\max} - d < 0\} \tag{57}$$

in which d is computed by [47]

$$d = \left(\sum_{i=1}^{6} \frac{N_i^0 N_i}{A_i} + \sqrt{2}\sum_{i=7}^{10} \frac{N_i^0 N_i}{A_i}\right)\frac{L}{E} \tag{58}$$

Table 5 Variables of Example 3

Variable	Parameter 1	Parameter 2	Distribution
A_1 (mm^2)	4000	50	Normal
A_2 (mm^2)	4000	50	Normal
A_3 (mm^2)	4000	50	Normal
A_4 (mm^2)	4000	80	Normal
A_5 (mm^2)	4000	80	Normal
A_6 (mm^2)	4000	80	Normal
A_7 (mm^2)	4000	100	Lognormal
A_8 (mm^2)	4000	100	Lognormal
A_9 (mm^2)	4000	100	Lognormal
A_{10} (mm^2)	4000	100	Lognormal
F_1 (N)	442,800	446,800	Interval
F_2 (N)	442,800	446,800	Interval
F_3 (N)	1709,200	1849,200	Interval

Table 6 Results of Example 3

Method	$[\underline{p}_f, \bar{p}_f]$	$[\underline{\varepsilon}, \bar{\varepsilon}]$ (%)	NOF
Random field	$[0, 4.153 \times 10^{-3}]$	[0, 1.49]	401
Direct Kriging	$[0, 3.88 \times 10^{-3}]$	[0, 5.18]	1000
Equivalent MPP	$[\text{N/A}, 4.82 \times 10^{-2}]$	[N/A, 1077.91]	605
MCS	$[0, 4.092 \times 10^{-3}]$	N/A	3×10^9

where

$$\begin{cases} N_1 = F_2 - \frac{\sqrt{2}}{2}N_8, N_2 = -\frac{\sqrt{2}}{2}N_{10} \\ N_3 = -F_1 - 2F_2 + F_3 - \frac{\sqrt{2}}{2}N_8 \\ N_4 = -F_2 + F_3 - \frac{\sqrt{2}}{2}N_{10} \\ N_5 = -F_2 - \frac{\sqrt{2}}{2}N_8 - \frac{\sqrt{2}}{2}N_{10}, N_6 = -\frac{\sqrt{2}}{2}N_{10} \\ N_7 = \sqrt{2}(F_1 + F_2) + N_8, N_8 = \frac{a_{22}b_1 - a_{12}b_2}{a_{11}a_{22} - a_{12}a_{21}} \\ N_9 = \sqrt{2}F_2 + N_{10}, N_{10} = \frac{a_{11}b_2 - a_{21}b_1}{a_{11}a_{22} - a_{12}a_{21}} \end{cases} \tag{59}$$

$$\begin{cases} a_{11} = \left(\frac{1}{A_1} + \frac{1}{A_3} + \frac{1}{A_5} + \frac{2\sqrt{2}}{A_7} + \frac{2\sqrt{2}}{A_8}\right)\frac{L}{2E} \\ a_{12} = a_{21} = \frac{L}{2A_5E} \\ a_{22} = \left(\frac{1}{A_2} + \frac{1}{A_4} + \frac{1}{A_6} + \frac{2\sqrt{2}}{A_9} + \frac{2\sqrt{2}}{A_{10}}\right)\frac{L}{2E} \\ b_1 = \left(\frac{F_2}{A_1} - \frac{F_1 + 2F_2 - F_3}{A_3} - \frac{F_2}{A_5} - \frac{2\sqrt{2}(F_1 + F_2)}{A_7}\right)\frac{\sqrt{2}L}{2E} \\ b_2 = \left(\frac{\sqrt{2}(F_3 - F_2)}{A_4} - \frac{\sqrt{2}F_2}{A_5} - \frac{4F_2}{A_9}\right)\frac{L}{2E} \end{cases} \tag{60}$$

and N_i^0, $i = 1, 2, \ldots, 10$, are obtained by plugging $F_1 = F_3 = 0$ and $F_2 = 1$ into Eqs. (59) and (60).

There are ten independent random variables and three interval variables as shown in Table 5. The parameters for constructing the Kriging models of $\beta(\mathbf{y})$ and $\rho(\mathbf{y}, \mathbf{y}')$ are also the same as those in Example 1. The RA results are provided in Table 6. For the direct Kriging model method, we used the HS method to generate 1000 training points, which were more than the training points used by the random field approach. This example again shows the high accuracy and efficiency of the random field approach.

6 Conclusions

Interval variables are usually used to model uncertainty with limited information. As a result, the probability of failure is also

an interval variable. Most of the RA methods for both random and interval variables rely on the global extreme values of a response with respect to interval variables. When the response is a nonlinear function of the interval variables, the accuracy and efficiency of RA are not good. This work shows that the response is a random field with respect to interval variables. From this perspective, the reliability or probability of failure can be redefined using a random field approach. The new definition allows for a new RA method that maps the random field response into a Gaussian field through the FORM. The Kriging model method is employed to determine the mean and autocorrelation functions of the Gaussian field, which is then expanded with a number of Gaussian variables. Then the bounds of the probability of failure are estimated by MCS.

The proposed method avoids global optimization with respect to interval variables and therefore avoids performing FORM on the extreme values of the response. In addition, the proposed method obtains the lower and upper bounds of the probability of failure simultaneously. As the three examples demonstrated, the proposed method is accurate and efficient.

It is critical to construct the models of the mean and autocorrelation functions of the Gaussian field. The Kriging method is used in this work for this task. Other surrogate model methods can also be employed. When the dimension of interval variables is high, the proposed method may not perform well, because the Kriging method may not be efficient for large-scale problems. A large number of interval variables, however, should be avoided, because this situation will cause too-conservative RA results. More information should be collected to reduce the number of interval variables. The future work in this area is the sensitivity analysis that identifies the most important interval variables, for which more information needs to be collected.

Although the FORM-based random field approach does not approximate the limit-state function with respect to interval variables, it linearizes the limit-state function with respect to the transformed random variables. Even though the accuracy of FORM is acceptable for many engineering problems, its error will be large if the limit-state function is highly nonlinear with respect to the transformed random variables. Future work is to use a more accurate and reliable method, such as the SORM, to replace FORM.

Acknowledgment

This material is based upon work supported by the National Science Foundation through Grant CMMI 1300870. The support from the Intelligent Systems Center (ISC) at the Missouri University of Science and Technology is also acknowledged.

References

[1] Du, X., Sudjianto, A., and Huang, B., 2005, "Reliability-Based Design With the Mixture of Random and Interval Variables," ASME J. Mech. Des., **127**(6), pp. 1068–1076.
[2] Hu, Z., and Du, X., 2012, "Reliability Analysis for Hydrokinetic Turbine Blades," Renewable Energy, **48**(1), pp. 251–262.
[3] Qiu, Z., and Wang, J., 2010, "The Interval Estimation of Reliability for Probabilistic and Non-Probabilistic Hybrid Structural System," Eng. Fail. Anal., **17**(5), pp. 1142–1154.
[4] Du, L., Youn, B. D., Gorsich, D., and Choi, K., 2006, "Possibility-Based Design Optimization Method for Design Problems With Both Statistical and Fuzzy Input Data," ASME J. Mech. Des., **128**(4), pp. 928–935.
[5] Mourelatos, Z. P., and Zhou, J., 2006, "A Design Optimization Method Using Evidence Theory," ASME J. Mech. Des., **128**(4), pp. 901–908.
[6] Pascual, B., and Adhikari, S., 2012, "Combined Parametric–Nonparametric Uncertainty Quantification Using Random Matrix Theory and Polynomial Chaos Expansion," Comput. Struct., **112**(1), pp. 364–379.
[7] Soize, C., 2005, "Random Matrix Theory for Modeling Uncertainties in Computational Mechanics," Comput. Methods Appl. Mech. Eng., **194**(12), pp. 1333–1366.
[8] Pellissetti, M., Capiez-Lernout, E., Pradlwarter, H., Soize, C., and Schueller, G., 2008, "Reliability Analysis of a Satellite Structure With a Parametric and a Non-Parametric Probabilistic Model," Comput. Methods Appl. Mech. Eng., **198**(2), pp. 344–357.
[9] Zaman, K., Rangavajhala, S., Mcdonald, M. P., and Mahadevan, S., 2011, "A Probabilistic Approach for Representation of Interval Uncertainty," Reliab. Eng. Syst. Saf., **96**(1), pp. 117–130.
[10] Xiao, N.-C., Huang, H.-Z., Wang, Z., Pang, Y., and He, L., 2011, "Reliability Sensitivity Analysis for Structural Systems in Interval Probability Form," Struct. Multidiscip. Optim., **44**(5), pp. 691–705.
[11] Bayarri, M. J., Berger, J. O., Paulo, R., Sacks, J., Cafeo, J. A., Cavendish, J., Lin, C.-H., and Tu, J., 2007, "A Framework for Validation of Computer Models," Technometrics, **49**(2), pp . 138–154.
[12] Jiang, C., Lu, G., Han, X., and Liu, L., 2012, "A New Reliability Analysis Method for Uncertain Structures With Random and Interval Variables," Int. J. Mech. Mater. Des., **8**(2), pp. 169–182.
[13] Jiang, C., Han, X., Li, W., Liu, J., and Zhang, Z., 2012, "A Hybrid Reliability Approach Based on Probability and Interval for Uncertain Structures," ASME J. Mech. Des., **134**(3), p. 031001.
[14] Adduri, P. R., and Penmetsa, R. C., 2007, "Bounds on Structural System Reliability in the Presence of Interval Variables," Comput. Struct., **85**(5), pp. 320–329.
[15] Luo, Y., Kang, Z., and Li, A., 2009, "Structural Reliability Assessment Based on Probability and Convex Set Mixed Model," Comput. Struct., **87**(21), pp. 1408–1415.
[16] Kang, Z., and Luo, Y., 2010, "Reliability-Based Structural Optimization With Probability and Convex Set Hybrid Models," Struct. Multidiscip. Optim., **42**(1), pp. 89–102.
[17] Penmetsa, R. C., and Grandhi, R. V., 2002, "Efficient Estimation of Structural Reliability for Problems With Uncertain Intervals," Comput. Struct., **80**(12), pp. 1103–1112.
[18] Zhang, H., Mullen, R. L., and Muhanna, R. L., 2010, "Interval Monte Carlo Methods for Structural Reliability," Struct. Saf., **32**(3), pp. 183–190.
[19] Du, X., Sudjianto, A., and Huang, B., 2005, "Reliability-Based Design With the Mixture of Random and Interval Variables," ASME J. Mech. Des., **127**(6), pp. 1068–1076.
[20] Guo, J., and Du, X., 2010, "Reliability Analysis for Multidisciplinary Systems With Random and Interval Variables," AIAA J., **48**(1), pp. 82–91.
[21] Choi, S.-K., Grandhi, R. V., and Canfield, R. A., 2007, *Reliability-Based Structural Design*, Springer, London.
[22] Zhuang, X., and Pan, R., 2012, "Epistemic Uncertainty in Reliability-Based Design Optimization," Proceedings of Reliability and Maintainability Symposium (RAMS), Reno, NV, Jan. 23–26, IEEE, pp. 1–6.
[23] Li, G., Lu, Z., Lu, Z., and Xu, J., 2014, "Regional Sensitivity Analysis of Aleatory and Epistemic Uncertainties on Failure Probability," Mech. Syst. Signal Process., **46**(2), pp. 209–226.
[24] Yoo, D., and Lee, I., 2013, "Sampling-Based Approach for Design Optimization in the Presence of Interval Variables," Struct. Multidiscip. Optim., **49**(2), pp. 253–266.
[25] Zhang, Y., and Hosder, S., 2013, "Robust Design Optimization Under Mixed Uncertainties With Stochastic Expansions," ASME J. Mech. Des., **135**(8), p. 081005.
[26] Adler, R. J., and Taylor, J. E., 2009, *Random Fields and Geometry*, Springer, New York.
[27] Sudret, B., and Der Kiureghian, A., 2000, "Stochastic Finite Element Methods and Reliability: A State-of-the-Art Report," Department of Civil and Environmental Engineering, University of California, Berkeley, CA.
[28] Hu, Z., and Du, X., 2015, "First Order Reliability Method for Time-Variant Problems Using Series Expansions," Struct. Multidiscip. Optim., **51**(1), pp. 1–21.
[29] Li, C.-C., and Der Kiureghian, A., 1993, "Optimal Discretization of Random Fields," J. Eng. Mech., **119**(6), pp. 1136–1154.
[30] Du, X., and Hu, Z., 2012, "First Order Reliability Method With Truncated Random Variables," ASME J. Mech. Des., **134**(9), p. 091005.
[31] Der Kiureghian, A., and Dakessian, T., 1998, "Multiple Design Points in First and Second-Order Reliability," Struct. Saf., **20**(1), pp. 37–49.
[32] Der Kiureghian, A., Zhang, Y., and Li, C.-C., 1994, "Inverse Reliability Problem," J. Eng. Mech., **120**(5), pp. 1154–1159.
[33] Sudret, B., and Der Kiureghian, A., 2002, "Comparison of Finite Element Reliability Methods," Probab. Eng. Mech., **17**(4), pp. 337–348.
[34] Kbiob, D., 1951, "A Statistical Approach to Some Basic Mine Valuation Problems on the Witwatersrand," J. Chem. Met. Min. Soc. S. Afr, **3**(1), pp. 201–215.
[35] Kaymaz, I., 2005, "Application of Kriging Method to Structural Reliability Problems," Struct. Saf., **27**(2), pp. 133–151.
[36] Xiong, Y., Chen, W., Apley, D., and Ding, X., 2007, "A Non-Stationary Covariance-Based Kriging Method for Metamodelling in Engineering Design," Int. J. Numer. Methods Eng., **71**(6), pp. 733–756.
[37] Kleijnen, J. P., 2009, "Kriging Metamodeling in Simulation: A Review," Eur. J. Oper. Res., **192**(3), pp. 707–716.
[38] Rasmussen, C. E., 2006, *Gaussian Processes for Machine Learning*, The MIT Press, Cambridge, MA, pp. 1–20.
[39] Santner, T. J., Williams, B. J., and Notz, W., 2003, *The Design and Analysis of Computer Experiments*, Springer, New York.

[40] Lophaven, S. N., Nielsen, H. B., and Søndergaard, J., 2002, "Dace-a Matlab Kriging Toolbox, Version 2.0," Technical Report.
[41] Echard, B., Gayton, N., and Lemaire, M., 2011, "Ak-Mcs: An Active Learning Reliability Method Combining Kriging and Monte Carlo Simulation," Struct. Saf., **33**(2), pp. 145–154.
[42] Bichon, B. J., Eldred, M. S., Swiler, L. P., Mahadevan, S., and Mcfarland, J. M., 2008, "Efficient Global Reliability Analysis for Nonlinear Implicit Performance Functions," AIAA J., **46**(10), pp. 2459–2468.
[43] Vitter, J. S., 1985, "Random Sampling with a Reservoir," ACM Trans. Math. Software (TOMS), **11**(1), pp. 37–57.
[44] Helton, J. C., and Davis, F. J., 2003, "Latin Hypercube Sampling and the Propagation of Uncertainty in Analyses of Complex Systems," Reliab. Eng. Syst. Saf., **81**(1), pp. 23–69.
[45] Hammersley, J. M., 1960, "Monte Carlo Methods for Solving Multivariable Problems," Ann. N. Y. Acad. Sci., **86**(3), pp. 844–874.
[46] Björkman, M., and Holmström, K., 1999, "Global Optimization Using Direct Algorithm in Matlab," Adv. Model. Optim., **1**(2), pp. 17–37
[47] Au, F., Cheng, Y., Tham, L., and Zeng, G., 2003, "Robust Design of Structures Using Convex Models," Comput. Struct., **81**(28), pp. 2611–2619.